

# Vorticity Generation in Slow Cooling Flows

Ami Glasner, Eli Livne, and Baruch Meerson

*The Racah Institute of Physics, the Hebrew University of Jerusalem, Jerusalem 91904, Israel*

We show that any generic non-adiabatic slow flow of ideal compressible fluid develops a significant vorticity. As an example, an initially irrotational conductive cooling flow (CF) is considered. A perturbation theory for the vorticity generation is developed that employs, as a zero order solution, a novel two-dimensional similarity solution. Full gasdynamic simulations of this CF demonstrate the vorticity generation and support the theory. The relevance of this problem to the experiments with the “hot channels” is discussed.

PACS numbers: 47.32.Cc, 47.40.Dc

The most general mechanism of the vorticity production in non-adiabatic flows of ideal compressible fluids relies on the misalignment of pressure and density gradients [1]. Recent experiments with supersonic flows [2,3] have clearly demonstrated the efficiency of this mechanism (which is called baroclinic). The baroclinic mechanism can also operate in slow gas flows, and its specific manifestations in meteorology [1] and combustion [4] are known. The main objective of this Letter is to show that the vorticity production represents a generic and significant property of *any* slow non-adiabatic gas flow.

For concreteness, we will consider the conductive cooling flows (CFs) and refer to the “hot channels” produced in the air by lasers or electric discharges [5,6]. After pressure equilibration these channels develop a significant vorticity and small scale turbulence and cool much faster than they would because of molecular thermal conduction. Picone and Boris [7] interpreted these results in terms of the baroclinic vorticity production *during the rapid channel expansion* (that is, on the acoustic time scale) [8]. Schlieren photographs of the hot channels [5,6] clearly show that the most significant vorticity dynamics occurs on a much longer time scale. According to Picone and Boris, “after pressure equilibration... vorticity is no longer generated, however, significant residual vorticity exists” [7]. We wish to present an alternative scenario which assumes that a significant vorticity is *created* on the long, heat-conduction time scale. The underlying physics is the following. After a few acoustic times, following the rapid energy release, the gas pressure becomes very close to the (constant) ambient pressure, while the vorticity generated earlier is presumably damped out. As the temperature inside the channel is still very high, a low-Mach-number conductive CF develops that cools the channel by filling it with the cold gas from the periphery. Slow conductive CFs were studied previously in the context of a “point-like” energy release, like a high-altitude explosion in the atmosphere [9] or “fireball” produced by a laser spark in front of condensed matter [10]. We will show that, unless the energy release geometry is *fully* symmetrical, small pressure gradients, intrinsic in the CF, result in a significant vorticity production.

The simplest conductive CF of a perfect gas is described by the standard gasdynamic equations [11]:

$$\frac{d\rho}{dt} + \rho \nabla \cdot \mathbf{v} = 0, \quad (1)$$

$$\epsilon^2 \rho \frac{d\mathbf{v}}{dt} = -\nabla p, \quad (2)$$

$$\gamma^{-1} \frac{dp}{dt} + p \nabla \cdot \mathbf{v} - \nabla \cdot (T^\nu \nabla T) = 0, \quad (3)$$

where  $d/dt = \partial/\partial t + \mathbf{v} \cdot \nabla$  is the total derivative. The distance is measured in the units of a characteristic spatial scale of the problem  $r_0$  (see later), while the time is measured in the units of the heat conduction time  $\tau_0 = \gamma(\gamma - 1)^{-1} R_g \rho_0 r_0^2 \kappa^{-1} T_0^{-\nu}$ . Furthermore, the gas density  $\rho$  and temperature  $T$  are scaled by their (presumably constant) values “at infinity”  $\rho_0$  and  $T_0$ , the velocity  $v$  is scaled by  $r_0/\tau_0$ , and the pressure  $p = \rho T$  is scaled by  $(R_g/\mu)\rho_0 T_0$ . The non-dimensional parameter  $\epsilon = r_0/c_s \tau_0$  (where  $c_s^2 = R_g T_0/\mu$ ) represents the characteristic Mach number of the flow. Finally,  $R_g, \gamma$  and  $\mu$  are the gas constant, adiabatic index and molar mass, respectively, while the heat conductivity is assumed to be a power-like function of the temperature:  $\kappa T^\nu$  in the scaled units,  $\kappa = \text{const.}$  (For the molecular air  $\nu = 1/2$ .)

We start with a perturbation theory that describes the initial stage of the vorticity production. Then we report on numerical simulations with the full equations (1)-(3) that show the vorticity generation in the same CF and support the theory.

In the low Mach number regime,  $\epsilon^2 \ll 1$ , the temperature and density contrasts can still be large, but pressure non-uniformities are already small:  $p(\mathbf{r}, t) = 1 + \epsilon^2 \delta p(\mathbf{r}, t)$ . Then, neglecting the small  $\delta p$  terms in Eq. (3) and equation of state, we obtain  $\nabla \cdot (\mathbf{v} - T^\nu \nabla T) = 0$  and  $\rho T = 1$ , respectively. It follows that  $\mathbf{v} = \mathbf{v}_p + \mathbf{v}_s$ , where  $\mathbf{v}_p = -\rho^{-\nu-2} \nabla \rho$  is the irrotational component of the fluid velocity, and  $\mathbf{v}_s$  is the solenoidal component:  $\nabla \cdot \mathbf{v}_s = 0$ . Substitution of  $\mathbf{v}$  into Eq. (1) yields a non-linear transport equation:

$$\frac{\partial \rho}{\partial t} + (\mathbf{v}_s \cdot \nabla) \rho = \nabla \cdot (\rho^{-\nu-1} \nabla \rho). \quad (4)$$

An important additional equation follows from Eq. (2):

$$\frac{\partial \vec{\omega}}{\partial t} - \nabla \times (\mathbf{v} \times \vec{\omega}) = \frac{d\mathbf{v}}{dt} \times \frac{\nabla \rho}{\rho}, \quad (5)$$

where  $\vec{\omega} = \nabla \times \mathbf{v} \equiv \nabla \times \mathbf{v}_s$  is the vorticity. Eq. (5) is equivalent to the well-known vorticity equation [1], as its right-hand-side can be rewritten as  $\nabla \rho \times \nabla \delta p / \rho^2$ . Note that Eq. (5) does not include  $\epsilon$ , therefore, the vorticity production rate is, in general, of order unity.

In this Letter we address the vorticity production in an initially curl-free flow. Accordingly, we assume that  $v_s \ll v_p$  and, in the zero order, neglect the second term in the left side of Eq. (4). The resulting nonlinear diffusion equation,

$$\frac{\partial \rho}{\partial t} = \nabla \cdot (\rho^{-\nu-1} \nabla \rho), \quad (6)$$

describes such a curl-free CF completely [9,10]. Now we consider a first-order version of Eq. (5), rewritten in terms of the vector field  $\mathbf{a}(\mathbf{r}, t) = \partial \mathbf{v}_s / \partial t$ :

$$\nabla \times \mathbf{a} + \frac{\nabla \rho}{\rho} \times \mathbf{a} = \left[ \frac{\partial \mathbf{v}_p}{\partial t} + (\mathbf{v}_p \cdot \nabla) \mathbf{v}_p \right] \times \frac{\nabla \rho}{\rho}, \quad (7)$$

with  $\rho$  and  $\mathbf{v}_p$  given by the curl-free solution [12]. Again, Eq. (7) shows that for a generic CF the vorticity production rate is of order unity. Therefore, the solenoidal part of the velocity field finally becomes comparable to its irrotational part (at which stage this perturbation scheme breaks down).

Let us concentrate on a two-dimensional (2d) flow in the  $xy$ -plane with no  $z$ -dependence, where one can produce the first two ‘‘classes of asymmetries’’ of the hot channels [7]: (i) off-center laser beam propagation and (ii) non-circular cross section of the beam. Introduce a modified stream function  $\psi(x, y, t)$ , so that  $a_x = -\partial \psi / \partial y$  and  $a_y = \partial \psi / \partial x$ . Eq. (7) becomes a scalar equation for  $\psi$ :

$$\nabla \cdot (\rho \nabla \psi) = \left[ \left( \frac{\partial \mathbf{v}_p}{\partial t} + (\mathbf{v}_p \cdot \nabla) \mathbf{v}_p \right) \times \nabla \rho \right] \cdot \mathbf{e}_z, \quad (8)$$

where  $\mathbf{e}_z$  is the unit vector in the  $z$ -direction.

One should, however, deal first with Eq. (6) and find the zero-order solutions  $\rho(x, y, t)$  and  $\mathbf{v}_p(x, y, t)$  entering Eq. (8). Remarkably, Eq. (6) has a family of 2d-similarity solutions of the second kind:

$$\rho(x, y, t) = t^{\frac{1-2\beta}{1+\nu}} R(\xi, \eta), \quad (9)$$

where  $\xi = x/t^\beta$ ,  $\eta = y/t^\beta$ , and  $\beta$  is an arbitrary real parameter [13]. Selection of parameter  $\beta$  requires the use of initial or boundary conditions. We shall adopt the following initial density profile:  $\rho(x, y, t = 0) = A^{-1} r^k f(\phi)$ ,

where  $r$  and  $\phi$  are the polar coordinates in the plane  $xy$ , and  $A$  and  $k$  are constants. In the case of a cylindrically-symmetric [ $f(\phi) = 1$ ] explosion along the  $z$ -axis, this profile with  $k = 2/(\gamma - 1)$  represents the  $r \rightarrow 0$  density asymptotics that sets in at the end of the expansion stage [14,15]. The function  $f(\phi)$  describes asymmetry. In analogy to Ref. [9], we extend this initial condition to the whole CF region. This idealization is justified (see Refs. [10,9] and gasdynamic simulations below) as long as the density (temperature) contrast in the system remains much larger than unity.

The initial condition yields  $\beta = (\nu k + k + 2)^{-1}$ . Using Eq. (9), one arrives at a nonlinear elliptic equation for the shape function  $R(\xi, \eta)$ :

$$\frac{\partial}{\partial \xi} \left( R^{-1-\nu} \frac{\partial R}{\partial \xi} \right) + \frac{\partial}{\partial \eta} \left( R^{-1-\nu} \frac{\partial R}{\partial \eta} \right) + (\nu k + k + 2)^{-1} \left( \xi \frac{\partial R}{\partial \xi} + \eta \frac{\partial R}{\partial \eta} - k R \right) = 0 \quad (10)$$

(we got rid of the constant  $A$  by choosing  $r_0 = A^{1/k}$ ). We assume for simplicity that the initial density profile [and, hence,  $R(\xi, \eta)$ ] is symmetric with respect to each of the Cartesian axes and solve Eq. (10) in the first quadrant with the no-flux boundary conditions at the  $\xi$ - and  $\eta$ -axes. In addition, we must require that  $R(\xi \rightarrow \infty, \eta \rightarrow \infty) = \hat{r}^k f(\hat{\phi})$ , where  $\hat{r}$  and  $\hat{\phi}$  are the polar coordinates in the plane  $\xi, \eta$ . Fig. 1 shows  $R(\xi, \eta)$  found numerically in a finite square for  $f(\hat{\phi}) = 1 + a \cos 2\hat{\phi}$ . We took the usual values  $\gamma = 1.4$  and  $\nu = 0.5$  for the molecular air, and chose  $a = 0.6$ . (In this case  $\beta = 2/19$ , while the gas density at the channel axis grows in time like  $t^{10/19}$ .)

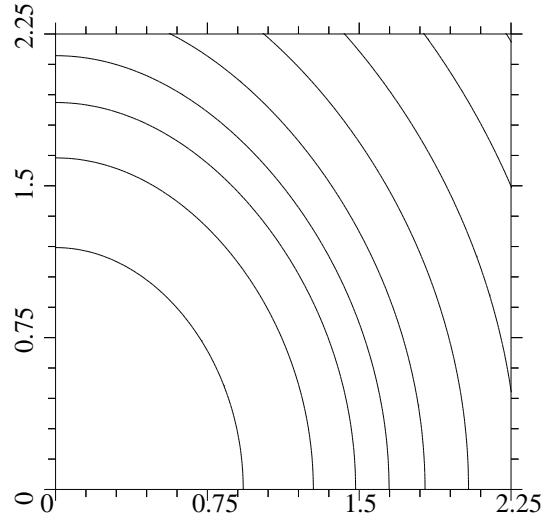


FIG. 1. Contours of  $\lg R(\xi, \eta)$ . On the inner line  $\lg R = 0.25$  and increases outwards in steps of 0.25. Also,  $R(0, 0) \approx 1.99$ .

Now we return to Eq. (8). A similarity solution for  $\rho$  implies a similarity solution for  $\psi$ , that is  $\psi(x, y, t) = t^{-\alpha} \Psi(\xi, \eta)$ , where  $\alpha = 2(\nu k + k + 1)/(\nu k + k + 2)$ . For

the shape function  $\Psi(\xi, \eta)$  one obtains a linear elliptic equation  $\nabla \cdot (R\nabla\Psi) = (\mathbf{W} \times \nabla R) \cdot \mathbf{e}_z$ , where

$$\mathbf{W} = -(\nu k + k + 2)^{-1} \left[ (\nu k + k + 1)\mathbf{V} + \xi \frac{\partial \mathbf{V}}{\partial \xi} + \eta \frac{\partial \mathbf{V}}{\partial \eta} \right] + (\mathbf{V} \cdot \nabla)\mathbf{V},$$

$\mathbf{V} = -R^{-\nu-2}\nabla R$ , and the  $\nabla$ -operator now involves differentiation with respect to  $\xi$  and  $\eta$ . This equation should be solved in the first quadrant with the Dirichlet boundary condition. We solved it numerically using the shape function  $R$  found earlier (in this case  $\alpha = 34/19 \approx 1.79$ ). The result is shown in Fig. 2. Now we can evaluate the vorticity  $\vec{\omega} = \omega(x, y, t)\mathbf{e}_z$ , using the relation  $(\partial\omega/\partial t)_{x,y} = \nabla^2\psi$ . Following Picone and Boris [7], we calculate the vorticity flux  $\Omega$  through the first quadrant as a function of time. The growth rate of this quantity,  $d\Omega/dt$ , is equal to

$$\int_0^\infty \int_0^\infty dx dy \nabla^2\psi = \oint_C (\nabla\psi \cdot \mathbf{n}) dl, \quad (11)$$

where  $C$  is the contour going from infinity to zero along the  $y$ -axis and continuing to infinity along the  $x$ -axis and  $\mathbf{n}$  is the external normal. Employing the similarity solution for  $\psi$ , we obtain

$$\frac{d\Omega}{dt} = -(t + t_0)^{-\alpha} \left[ \int_0^\infty \frac{\partial\Psi}{\partial\xi}(0, \eta) d\eta + \int_0^\infty \frac{\partial\Psi}{\partial\eta}(\xi, 0) d\xi \right], \quad (12)$$

where we have used the invariance of the similarity solution with respect to a time shift and introduced  $t_0$ , the only fitting parameter of the theory. Integrating Eq. (12) with a zero initial condition, we arrive at

$$|\Omega(t)| = |B| (\alpha - 1)^{-1} [t_0^{1-\alpha} - (t + t_0)^{1-\alpha}], \quad (13)$$

where  $B$  is the constant given by the expression in the square brackets in Eq. (12). Eq. (13) predicts a linear growth of  $\Omega$  with time followed by saturation at a constant value  $|B| (\alpha - 1)^{-1} t_0^{1-\alpha}$ .

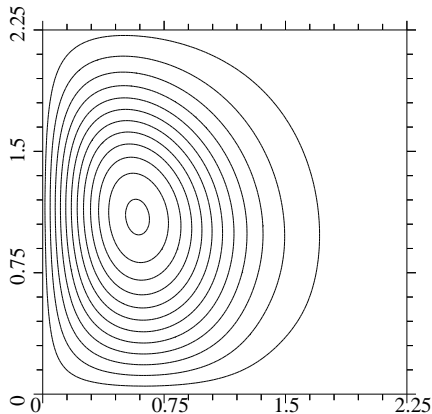


FIG. 2. Contours of  $\Psi(\xi, \eta)$ . On the outer line  $\Psi = 10^{-4}$  and increases inwards in steps of  $10^{-4}$ .

Now we report on the 2d-numerical simulations with Eqs. (1)-(3). We employed an extended version of the code VULCAN [16] that uses flexible moving grids and can operate in any combination of Eulerian and Lagrangian modes. In the rezoning stage we used the scheme of Van Leer [17] that preserves second order accuracy. The code could work in an implicit mode, thus eliminating the Courant-Friedrichs-Lewy restriction on the time step. The initial conditions were

$$\rho(r, \phi, t = 0) \equiv \rho_{in} = \frac{\delta + r^k(1 + a \cos 2\phi)}{1 + r^k(1 + a \cos 2\phi)}, \quad (14)$$

for the density,  $\mathbf{v}(r, \phi, t = 0) = -\rho_{in}^{-\nu-2}\nabla\rho_{in}$  for the velocity, and unity for the pressure. For  $\delta \ll 1$ , the initial density profile has an extended part described by  $r^k(1 + a \cos 2\phi)$  (which yields the 2d-similarity solution). On the other hand,  $\rho_{in}$  is non-zero at  $r = 0$  and approaches unity at  $r \rightarrow \infty$  as it should. In most of simulations we took  $\delta = 10^{-2}$ ,  $a = 0.6$  and  $\epsilon$  in the range of  $10^{-6}$  to  $10^{-5}$ . Simulations show that the density history at the channel axis is described very well by the similarity scaling  $1.99(t + 4.2 \times 10^{-5})^{10/19}$  until the late stage, when the density contrast is reduced. However, the velocity field (that was curl-free in the beginning, Fig. 3a) develops a noticeable vorticity which spatial structure is similar to that shown in Fig. 2. Finally, a distinctive vortex, advected towards the origin by the overdense gas inflow, appears (Fig. 3b). Since the problem is symmetric with respect to each of the axes, the corresponding "full" flow develops four symmetric vortices. Fig. 4 shows the time history of the vorticity flux through the first quadrant,  $\Omega$ , as found from the simulations. It is seen that the vorticity reaches a significant value. One can also see that the perturbation theory [Eq. (13)] underestimates the saturated vorticity flux. This is understandable, as the perturbation scheme fails at large times. Interestingly, the agreement improves for a smaller value of  $t_0$ .

In summary, we claim that any generic non-adiabatic gas flow develops a significant vorticity. For the low-Mach-number conductive CF that we have considered in detail, the further vorticity dynamics (instability?) is apparently sensitive to geometry (like in the Picone-Boris scenario). We did not observe turbulence or other significant modification of the bulk transport properties in this (still highly symmetric) 2d-flow. Correspondingly, the "hot channel" riddle requires further investigation. One can expect turbulence to show up in a less symmetric 3d situation, when perturbations along the channel axis are introduced.

B.M. acknowledges a valuable discussion with P.V. Sasorov.

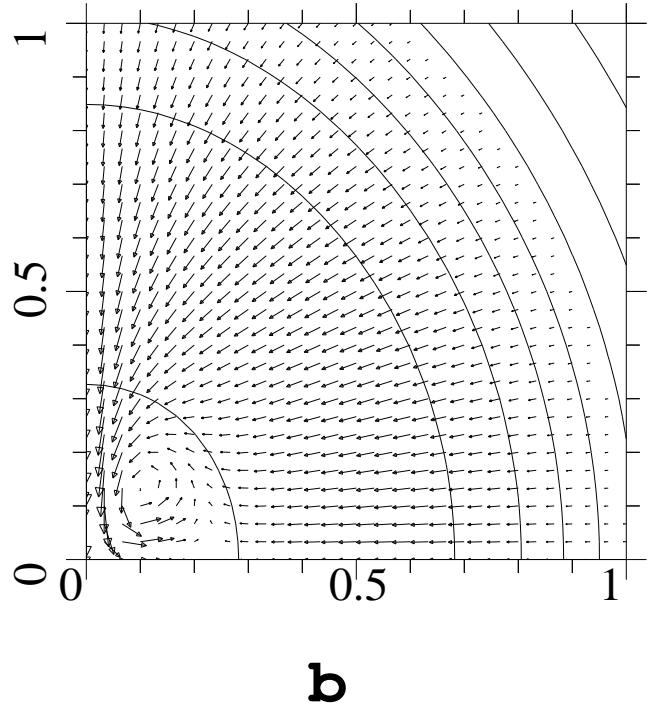
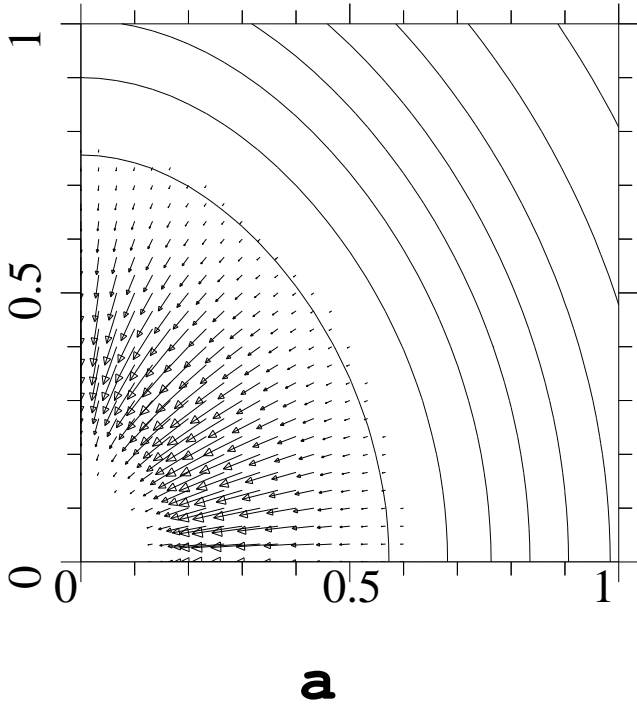


FIG. 3. Density and velocity fields at  $t = 0$  (a) and  $t = 3 \times 10^{-3}$  (b). The velocity field (arrows) is scaled by 3000 (a) and 100 (b). On the inner density isolines  $\rho = 0.1$  and increases outwards in steps of 0.1.

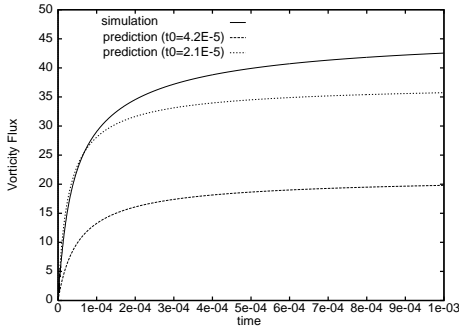


FIG. 4. Vorticity flux through the first quadrant vs time, as predicted by the full simulations, and by Eq. (13) with different values of  $t_0$ .

- 
- [1] J. Pedlosky, *Geophysical Fluid Dynamics* (Springer, New York, 1987).
  - [2] J. Grun *et al.*, Phys. Rev. Letters **66**, 2738 (1991); NRL Memo No. 7366 (1993).
  - [3] J.W. Jacobs *et al.*, J. Fluid Mech. **295**, 23 (1995).
  - [4] T. Miyauchi, and M. Tanahashi, in *Modeling in Combustion Science*, edited by J. Buckmaster and T. Takeno (Springer, Berlin, 1995), p. 47.
  - [5] J.R. Greig *et al.*, Phys. Rev. Lett. **41**, 174 (1978).
  - [6] J.M. Picone *et al.*, J. Atmos. Sci. **38**, 2056 (1981).
  - [7] J.M. Picone, and J.P. Boris, Phys. Fluids **26**, 365 (1983).
  - [8] More recently, the Rayleigh-Taylor instability of the shock underpressure air flowing into the channel was suggested as an alternative scenario [R.D. Hill, Phys. Fluids B **3**, 1787 (1991)], but still operating during the rapid stage.
  - [9] B. Meerson, Phys. Fluids A **1**, 887 (1989).
  - [10] D. Kaganovich *et al.*, Phys. Plasmas **3**, 631 (1996).
  - [11] L.D. Landau and E.M. Lifshitz, *Fluid Mechanics* (Pergamon, New York, 1987).
  - [12] Only those first-order terms in  $\mathbf{v}_s$  that include  $\mathbf{a}$  are kept in Eq. (7), as they are not small already at  $t = 0$ .
  - [13] In three dimensions, the corresponding similarity solutions have an additional argument  $z/t^\beta$ .
  - [14] Ya. B. Zel'dovich and Yu. P. Raizer, *The Physics of Shock Waves and High Temperature Hydrodynamic Phenomena* (Academic, New York, 1967).
  - [15] V.P. Korobeinikov, *Problems in the Theory of Point Explosion in Gases* (AMS, Providence, Rhode Island, 1976).
  - [16] E. Livne, Ap. J. **412**, 634 (1993).
  - [17] B. Van Leer, J. Comput. Phys. **32**, 101 (1979).